euspen's 25th International Conference & Exhibition, Zaragoza, ES, June 2025
www.euspen.eu

Spherical Tulip Electrical Contacts for Quasi Kinematic Coupling of Rapid Swap Batteries

Abigail Wucherer[1], David Edington[1], Aditya Mehrotra[1], Alexander Slocum[1]

[1]*Department of Mechanical Engineering, Massachusetts Institute of Technology*

Abigail2@mit.edu

Abstract
In the drive towards a globally decarbonized energy economy, rapid swap battery packs provide a potential means to improve electric vehicle adoption in high utilization industrial vehicles where lengthy charge times are a barrier to electrification. High voltage, high current battery connectors are a critical component for coupling the pack to the electric vehicle, distributing power from the battery to the drivetrain. Introduced here is a quasi-kinematic coupling-based connector with integrated electrical contacts, allowing for repeatable and accurate positioning of the battery pack to the vehicle. A slotted ball and socket design approach is considered to accommodate for angular misalignment and establish high contact area through elastic averaging. Contact resistance, a primary metric for evaluating the functionality of an electrical contact, is explored as a function of scrub, contact area, and compliance within the connector. Initial characterization of wear is also evaluated for identifying failure mechanisms and to validate the design strategy of encouraging relative sliding motion at the contact interface to break through the continuously re-formed oxide layers on each mating cycle for improved conductivity.

Kinematic coupling, contact resistance, elastic averaging, electric vehicles

1. Introduction

According to the U.S. Energy Information Administration, the transportation sector will be responsible for the most emission reductions from now till 2030 with the goal of Net Zero by 2050 [1]. Swappable battery systems address the challenge of prolonged charging times for heavy-duty and high utilization vehicles such as those used in industrial applications, public transportation, autonomous taxis, and warehouse robotics [2,3]. Additionally, swappable batteries create economic opportunities for both the vehicle owner and battery pack owner. Decoupling the ownership allows for vehicles to outlive the battery pack and the costs to be made independent. Battery packs have a finite lifespan, with cell degradation from cycling, energy, and power requirements leading to reduced cycle life and reliability over time [4,5], so at the battery's end of life, the entire vehicle must be replaced [4,6]. Swappable systems also help alleviate the strain on the power grid by mitigating demand surges from fast charging and enabling batteries to be charged slower and during off-peak, lower-cost times [3,7]. These systems offer a more efficient and economical approach to full electrification of the transportation sector.

A significant barrier to swappable battery technology is a reliable and scalable design for the electrical and mechanical interface between the pack and vehicle. Simply scaling existing swappable battery connectors is not viable because as technology scales in size, attainable precision decreases. Locating, inserting, and mitigating damage to the connector becomes more challenging in larger systems.

Commonly found, tulip connectors and pin-and-socket connectors comprised of curved leaf springs mating with rigid surfaces [8] are often utilized in medium to high-voltage applications [9]. While these designs meet current and voltage specifications, they can be limited by cycle life and cost.

To address these challenges, this work combines principles of precision mechanical design and electrical contact design to deliver a scalable rapid swap battery connector achieving reliable operation in large systems. This work utilizes a modified Quasi-Kinematic Coupling (QKC) for precision alignment and repeatability, establishing arc line contact through elastic averaging [10,11]. This creates a design space where weight, geometry, and contact resistances can be optimized by integrating both structural and electrical capabilities within a single connector.

Measuring contact resistance is the most significant metric for evaluating performance of an electrical connector [12, 13]. From a systems-level design perspective, increasing the contact force and incorporating scrub—relative sliding motion between surfaces—are effective strategies for reducing and maintaining low contact resistance [12]. Design strategies to reduce contact resistance and wear rates are also presented and tested in this work.

2. System Requirements

Rapid swap battery systems rely on the ability to reliably align, engage electrical connectivity, and lock the battery pack to the vehicle. These three requirements are intrinsic to the structural quasi-kinematic coupling for the electrical contact.

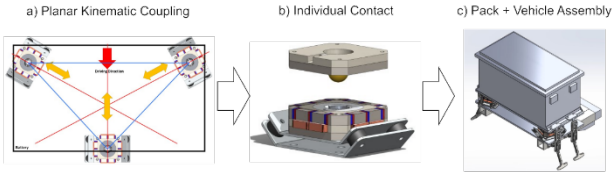

Figure 1. (Align (a), Engage (b), Lock (c)

The quasi-kinematic coupling design in (a) of Fig. 1. allows for precision alignment through its triangular configuration of the electrical contacts. The (b) section shows the engagement of the electrical contact which may be locked in place by a semi-permanent electromagnet ring configuration surrounding the ball and socket center for a tight structural loop. The weight of the battery pack in (c) preloads the contact to ensure electrical engagement, even without the locking mechanism. Ultimately, the system may be locked in place via pneumatic, hydraulic, or magnetic clamping systems.

3. Design For Electrical and Structural Performance

Contact resistance can be reduced through three focused areas: decreasing the intersection angle, establishing sufficient scrub- relative sliding motion between the plug and socket, and increasing the normal force across the interface.

3.1. Modified Ball and Socket Design

Six points of contact are established for exact constraint design, and can be accomplished through a curved "V-shape" design with six regions of line contact, but this design is susceptible to point loading and arcing with the presence of any system level misalignment [10]. To mitigate misalignment consequences, a ball and socket are used to accommodate angular misalignment and establish conformal contact [14,15]. Additionally, as a ball and socket joint wears, the contact pressure and wear rate decreases [16,17]. Initially, the repeated placement of the ball in the socket causes a high wear rate as the contact patch is established. As the contact patch expands, the contact pressure decreases, increasing the lifetime of an electrical contact.

The ball and socket interfaces are modified with slots to introduce compliant "petals." This modified coupling achieves low contact resistance by establishing scrub, repeatable contact area, and sufficient normal force at the interface.

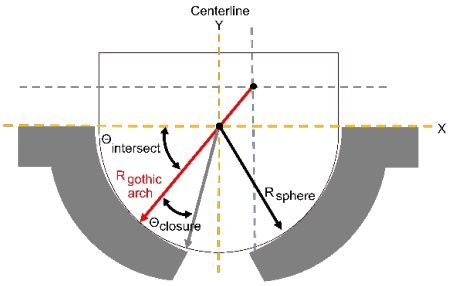

Figure 2. Gothic Arch for Revolving Around Centerline

For the QKC contactor socket design, the convex surfaces of revolution were chosen to be gothic arches revolved around the ball's center line [11]. The gothic arches have input parameters in Fig. 2 for fully constraining a two-dimensional cross section. The intersection angle, $\theta_{intersect}$, and ratio between the curved surface radii are primarily used to define the model. The intersection angle outlined in Fig. 2 is a design parameter for increasing the contact area. A lower intersection angle results in a larger circumference and higher force thus affecting contact pressure and contact resistance.

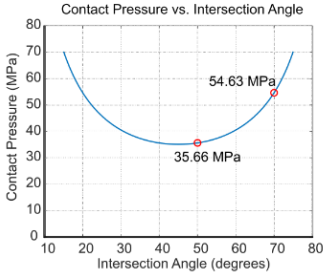

Figure 3. Contact Pressure vs. Intersection Angle

The contact pressure is a minimum at an intersection angle of 45 degrees as seen in Fig.3, suggesting that this angle may be the most ideal for reducing wear and establishing low contact resistance. As the intersection angle decreases, the force normal to the contact patch increases, thus decreasing contact resistance.

The closing angle of the gothic arch, $\theta_{closure}$, is defined as 5 degrees. This allows for a contact patch to be established in a practical sense without edge loading the gothic arch coincident with the intersection point, risking increased wear.

The radius ratio, $R_r=R_{gothicarch}/R_{sphere}$, was also anticipated to affect the contact area. By increasing the radius ratio of the socket, R_r, from 1 to 1.4, the contact area will decrease based on Hertz contact theory - a simplification of the system for the purpose of evaluating the impact of radius ratio on contact area [15]. This work evaluates distinct radius ratios of 1.1 and 1.4 to explore these effects further and allow for flexibility in alignment of the ball and socket during mating.

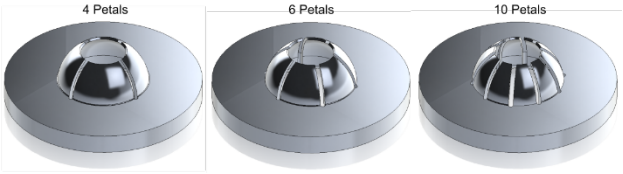

Figure 4. Petal Number Variations in Socket Design

Scrub is achieved by introducing stress relief slots in the revolved gothic arch socket. The quantity of these slots (Fig. 4) was chosen in efforts to increase scrub (Fig. 5) and decrease the maximum bending stress in the gothic arch petals.

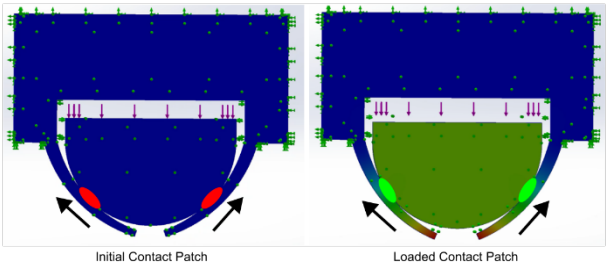

Figure 5. Movement of contact patch corresponding to scrub distance

Because increasing the normal force decreases the contact resistance, ensuring a reasonable normal force is achieved while not over stressing the contact is a critical to this design. Therefore, the socket with petals is supported by a flange that will contact a mating hard stop flange backing the ball (Fig. 6).

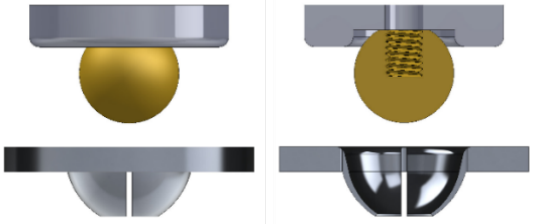

Figure 6. Ball and Socket Flange Mount

As the ball and socket are pressed together, the flanges will eventually contact resulting in a hard stop. When fully loaded, the flanges will act as the structural support for higher load bearing capacity. The normal force across the ball and socket will be a repeatable and fixed value allowing for optimization to reduce contact resistance while ensuring performance longevity.

4. Test Setup for Evaluating Design Parameter Impact

Experimental goals included:

1. Characterize the minimum scrub distance required to break the oxide layer.
2. Characterize design parameter relationships such as radius ratio, intersection angle, and petal number on contact resistance and contact area.
3. Compare the resistivity to commercial high voltage battery contacts to this connector.
4. Identify early risks in contact resistance variation with mechanical mating cycles.

Design parameters of intersection angle, radius ratio, and number of petals were anticipated to impact contact resistance and scrub. Scrub was verified by markings on the surface of the flower connector sample from optical microscope images and profilometer data. Additionally, scrub was measured indirectly by measuring the relative vertical movement between the ball and sample using an extensometer. Socket samples were CNC turned 6061 Al with milled slots, chosen for machining ease and low resistivity. Ultimately, the socket parts may be stamped for high volume manufacturing. Alternative materials and coatings for lower resistivity and resilience to wear should also be considered. The mating ball was a mirror polished 260 Brass.

Table 1 Test Sample Configurations

Sample ID	Intersection Angle	Radius Ratio	Number of Petals
1A	50	1.1	4
2A	50	1.1	6
3A	50	1.4	4
4A	50	1.4	6
5A	70	1.1	4
6A	70	1.1	6
7A	70	1.4	4
8A	70	1.4	6

A higher intersection angle was anticipated to increase the contact area but decrease expected scrub under a fixed force due to a higher stiffness. A higher radius ratio was expected to increase conformity, resulting in a greater contact area and decrease stiffness thus allowing for more scrub for a fixed force. A higher number of petals was expected to lower the contact area due to the contact area loss of the space between petals but increase the expected scrub due to a decrease in stiffness. The minimum required scrub to establish strong electrical contact was not established prior to experimentation, so minimum required scrub was of concern.

The test setup (Fig. 7) utilized a four wire method [13] for measuring electrical contact resistance with a DMM7510 7.5 Digit Graphical Sampling Multimeter from Tektronix. The Instron 5969 ramp rate was chosen to be 177.93 N/min (40 lbs/min) with a maximum loading of 177.93 N (40 lbs). The sample was preloaded to a force within 13.34 to 22.24 N (3- 5 lbs). A static axial clip-on extensometer was used to measure displacement.

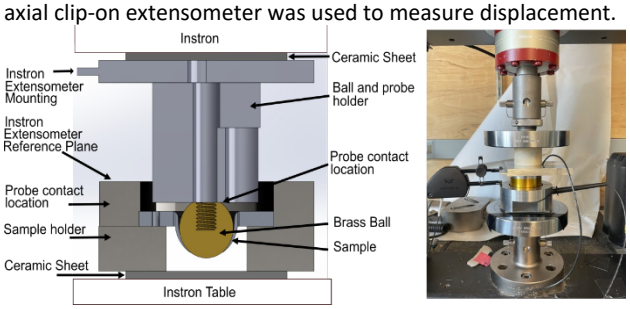

Figure 7. Instron Test Fixture

5. Test Results

For each of these samples, the minimum amount of scrub necessary to break the oxide layer was achieved, so there were no additional benefits to contact resistance from increasing the scrub distance. Extensometer data, the approximation for scrub, was compared across design configurations in Fig. 8, revealing this relationship.

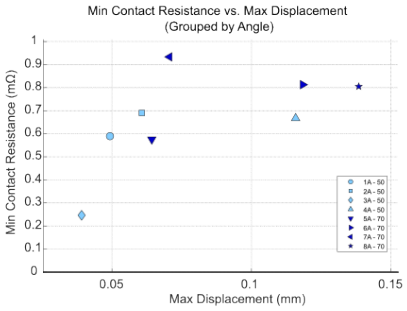

Figure 8. Minimum Contact Resistance vs. Maximum Displacement

Even the sample with the minimum scrub distance of 0.0381 mm (0.0015 in) established adequate contact to break the oxide layer. This indicates that the contact resistance is more so affected by the contact force than scrub distance for this design.

The contact resistance for each of the contacts was plotted against the applied load and grouped by design parameter to understand the impact of each variable on the contact resistance. As visible in Fig. 9 a higher contact angle resulted in a higher minimum contact resistance throughout the loading cycle on average. This can be explained by the increase in force normal to the contact patch at lower contact angles, confirming that the increased force is a driving factor in reducing contact resistance.

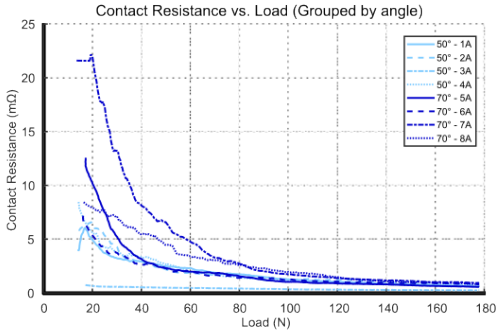

Figure 9. Contact Resistance Versus Load – Single Cycle

To investigate if increasing the intersection angle increased contact resistance a statistically significant amount, a two-sample unpaired t-test was used to evaluate the difference between the two-sample group mean values for the minimum contact resistance. A t-score of 1.8356 and one-tailed p-Value of .0664 was achieved. At a confidence level of 0.10, this is statistically significant such that the minimum contact resistance decreases with a lower intersection angle.

Grouping by radius ratio did not have a statistically significant impact on the contact resistance, with minimal change in the minimum contact resistance. This may be explained by the increase in contact area from a higher radius ratio having a negligible impact on contact resistance.

When grouping by the number of petals, the four-petal group on average had a lower contact resistance of 0.253 Ohms compared to their six-petal paired counterpart, but this yielded a p-value of 0.133 for a one-sided t-test. At a confidence level of 0.1, this result is not statistically significant, but could suggest stiffness increases from a four-petal configuration may improve the minimum achievable contact resistance.

The contact resistance and load data from repeatedly cycling the contacts showcased the importance of fully lifting the contact between loading to gain the benefits of scrub (Fig. 10 and 11). Across all samples, initially the minimum contact resistance from each compression cycle increased with the subsequent cycle- a result of not fully lifting the contact between cycles, just reducing the loading to near zero. However, this

geometry did show a reduction in minimum contact resistance from the first ever compression to the second. This may be explained by the anticipated asperity flattening. However, asperity flattening is different from some scrub features which may cause ridges as seen in Fig. 11. The average reduction in contact resistance was 0.378 mOhm from the first compression to the second compression.

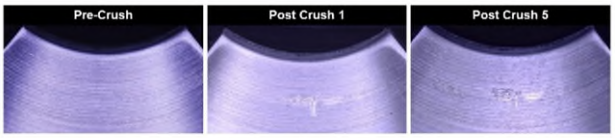

Figure 10. Optical evidence of scrub on sample 3A

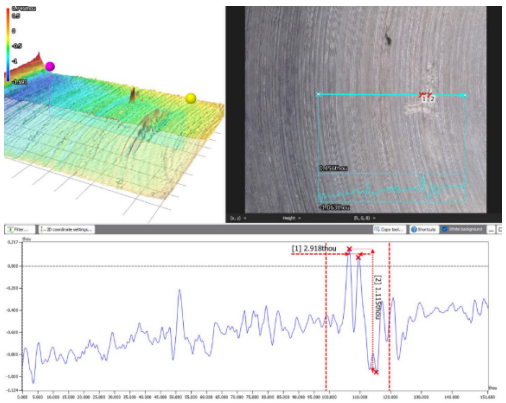

Figure 11. Keyence VK Profilometer evidence of scrub on sample 3A

This testing was then repeated with a full disconnection and mating of the ball and socket during 10 cycle compression testing. These results showed a leveling of contact resistance during testing, confirming that with sufficient scrub, this geometry can achieve consistent contact resistance performance as seen in Fig. 12.

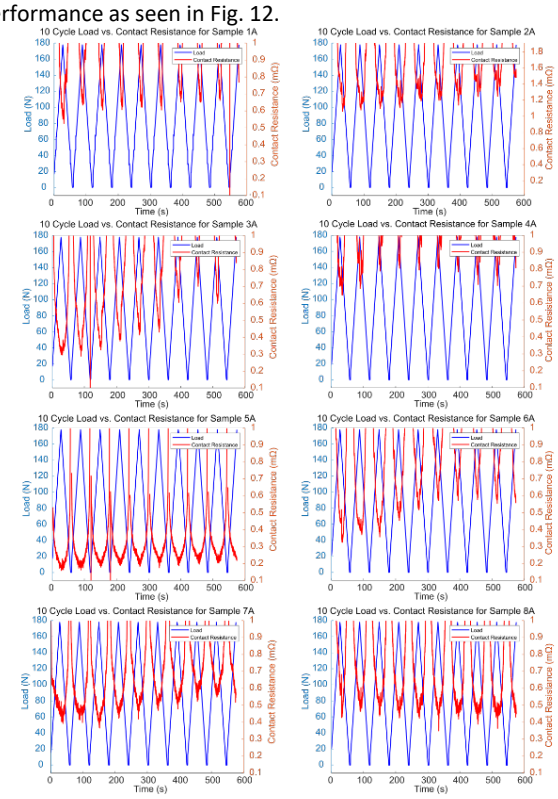

Figure 12. 10 Cycle Contact Resistance and Loading Results

6. Conclusions

This study introduced a coupled mechanical and electrical interface to enable reliable and repeatable placement of a battery pack on a vehicle, while achieving consistently low contact resistance during preliminary testing.

While the development of a closed-form solution for this design methodology remains ongoing, initial analytical results suggest effective strategies for tuning key design parameters to promote scrub behavior and ensure sufficient contact pressure for low contact resistance.

Experimental validation on a small electric vehicle confirmed the repeatability and stability of the interface, with low contact resistance maintained during repeated placement and removal of the battery pack and under typical driving conditions. Notably, the interface exhibits a wear-in period, during which the contact characteristics evolve. Long-term high-cycle testing is currently underway to quantify the wear-in cycle count, and this process is anticipated to improve the electrical stability of the interface, ensuring consistent and robust electrical contact over extended use.

References

[1] M. Huismans, F. Voswinkel, Electrification – energy system (2023)

[2] B. Subirana, M. Puig, S. Sarma, Can small smart swappable battery evs outperform gas powertrain economics?, IEEE 20th International Conference on Intelligent Transportation Systems, (2017)

[3] C. J. Chou, S. B. Jiang, T. L. Yeh, C. C. Sun, Fault-tolerant battery power network architecture of networked swappable battery packs in parallel, *Energies* **14** (2021)

[4] D. Wang, J. Coignard, T. Zeng, C. Zhang, S. Saxena, Quantifying electric vehicle battery degradation from driving vs. vehicle-to-grid services, *Journal of Power Sources* **332** (2016) 193-203.

[5] T. Yu, X. Li, B. Wang, W. Shi, Quantitative analysis of factors contributing to driving range degradation of battery electric vehicles, *APPLIED THERMAL ENGINEERING* **250** (2024).

[6] W. Diao, J. Jiang, C. Zhang, H. Liang, M. Pecht, Energy state of health estimation for battery packs based on the degradation and inconsistency, *Energy Procedia* **142** (2017) 3578–3583.

[7] P. Renna, S. Materi, Peak energy reduction in flow shop including switch-off policies and battery storage, *APPLIED SCIENCES-BASEL* **12** (2022).

[8] B. Ravelo, Multiphysics analysis of pin-socket electrical dynamic Contact susceptibility under vibration stress, *IEEE Transactions on Electromagnetic Compatibility* **61** (2019) 344-351.

[9] L. Boget, J.-B. Jourjon, European patent application 17290065.6; tulip-type electrical contact comprising a pressing element pressing on the conducting fingers at rest (2017).

[10] A. Slocum, Kinematic couplings: A review of design principles and applications, *International Journal of Machine Tools and Manufacture* 50 (2010)

[11] M. Culpepper, Design and application of compliant quasi-kinematic couplings, Phd thesis, Massachusetts Institute of Technology, Cambridge, MA, available at https://pergatory.mit.edu/kinematiccouplings/documents/Theses/culpepper thesis/quasi kinematic couplings.pdf (February 2000).

[12] P. G. Slade (Ed.), Electrical Contacts: Principles and Applications, Second Edition, CRC Press, 2014.

[13] W. Ren, D. Du, Y. Du, Electrical contact resistance of connector response to mechanical vibration environment, IEEE Transactions on Components, *Packaging and Manufacturing Technology* **10** (2020) 212-219.

[14] Z. Sun, C. Hao, Conformal contact problems of ball-socket and ball, Physics Procedia 25 (2012) 209–214, international Conference on Solid State Devices and Materials Science, April 1-2, 2012, Macao.

[15] C. S. Liu, K. Zhang, L. Yang, Normal force-displacement relationship of spherical joints with clearances, *Journal of Computational and Nonlinear Dynamics* **1** (2006) 160–167.

[16] R. Lee, A. Wang, A. Essner, S. Ge, Tribology of metal-on-metal bearings at high inclination angles, Advanced Tribology, Springer Berlin Heidelberg, 2010, pp. 24–25.

[17] M. Harun, F. Wang, Z. Jin, J. Fisher, Long-term contact-coupled wear pre-diction for total metal-on-metal hip joint replacement, Proceedings of the Institution of Mechanical Engineers, *Part J: Journal of Engineering Tribology* **223** (2009).